

Global and Regional Projected Changes in 100-yr Subdaily, Daily, and Multiday Precipitation Extremes Estimated from Three Large Ensembles of Climate Simulations

JEAN-LUC MARTEL

École de Technologie Supérieure, Université du Québec, Québec, Canada

ALAIN MAILHOT

Institut National de la Recherche Scientifique-Eau, Terre et Environnement, Québec, Canada

FRANÇOIS BRISSETTE

École de Technologie Supérieure, Université du Québec, Québec, Canada

(Manuscript received 7 November 2018, in final form 11 July 2019)

ABSTRACT

Many studies have reported projected increases in the frequency and intensity of extreme precipitation events in a warmer future climate. These results challenge the assumption of climate stationarity, a standard hypothesis in the estimation of extreme precipitation quantiles (e.g., 100-yr return period) often used as key design criteria for many infrastructures. In this work, changes in hourly to 5-day precipitation extremes occurring between the 1980–99 and 2080–99 periods are investigated using three large ensembles (LE) of climate simulations. The first two are the global CanESM2 50-member ensemble at a 2.8° resolution and the global CESM1 40-member ensemble at a 1° resolution. The third is the regional CRCM5 50-member ensemble at a 0.11° resolution, driven at its boundaries by the 50-member CanESM2 ensemble over the northeastern North America (NNA) and Europe (EU) domains. Results indicate increases in the frequency of future extreme events, and, accordingly, a reduction of the return period of current extreme events for all tested spatial resolutions and temporal scales. Agreement between the three ensembles suggests that extreme precipitations, corresponding to the 100-yr return period over the reference period, become 4–5 (2–4) times more frequent on average for the NNA (EU) domain for daily and 5-day annual maximum precipitation. Projections by CRCM5-LE show even larger increases for subdaily precipitation extremes. Considering the life-span of many public infrastructures, these changes may have important implications on service levels and the design of many water infrastructures and for public safety, and should therefore be taken into consideration in establishing design criteria.

1. Introduction

Daily and subdaily extreme precipitation events are of high importance when considering the design of public water infrastructures with long life expectancy. Due to

the relatively short observational records and rarity of such events, methods based on the statistical theory of extreme value have traditionally been used to estimate high precipitation quantiles (e.g., the 100-yr return period; Katz 2013; Schulz and Bernhardt 2016). However, actual design criteria generally assume that the climate is stationary, ignoring the scientific evidence pointing to human-induced global warming (Katz 2013; Mailhot and Duchesne 2010; Milly et al. 2008). It is expected that projected increases in global temperature will lead to an increase in the intensity of extreme rainfall events, partly because a warmer atmosphere can hold more moisture (IPCC 2013; Lenderink and Fowler 2017; Trenberth 1999; Trenberth et al. 2003). However, the relationship between the increase in temperature and

Denotes content that is immediately available upon publication as open access.

Supplemental information related to this paper is available at the Journals Online website: <https://doi.org/10.1175/JCLI-D-18-0764.s1>.

Corresponding author: Jean-Luc Martel, jean-luc.martel.1@ens.etsmtl.ca

DOI: 10.1175/JCLI-D-18-0764.1

© 2020 American Meteorological Society. For information regarding reuse of this content and general copyright information, consult the AMS Copyright Policy (www.ametsoc.org/PUBSReuseLicenses).

the projected change in extreme precipitation, especially at the subdaily scale, has been shown to be rather complex (Lenderink and Fowler 2017; Lenderink et al. 2011; Prein et al. 2017; Westra et al. 2014; Zhang et al. 2017).

Many studies, using various trend detection methods (Min et al. 2011; Westra et al. 2013) and datasets (Alexander et al. 2006; Donat et al. 2013b), have found that about two-thirds of the data-covered global land areas exhibit positive trends in annual daily precipitation extremes for the latter half of the twentieth century. Significant increases of various precipitation extremes indices have also been reported (Easterling et al. 2000; Groisman et al. 2005; Madsen et al. 2014; Seneviratne et al. 2012; Trenberth et al. 2007). Increasing trends in daily precipitation extremes were observed for the eastern half of North America (Donat et al. 2013b; Easterling et al. 2000; Groisman et al. 2005). Similar increases over many regions of Europe, notably over eastern and northern Europe, were also reported while decreases were observed in southern Europe and around the Mediterranean Basin (Donat et al. 2013b; Easterling et al. 2000; Groisman et al. 2005; Madsen et al. 2014; van den Besselaar et al. 2013; Zolina 2012).

There is also evidence, as highlighted in reviews by Westra et al. (2014) and Madsen et al. (2014), that anthropogenic climate change is also likely leading to an increase in recorded subdaily precipitation extremes. For instance, studies showed increases for durations ranging from multiple hours to days for North America (Brommer et al. 2007; Burn et al. 2011; Kunkel et al. 2013; Muschinski and Katz 2013) and for Europe (Arnone et al. 2013; Leahy and Kiely 2011; Madsen et al. 2009; Ntegeka and Willems 2008; Wang et al. 2011).

The Intergovernmental Panel on Climate Change (IPCC) Fifth Assessment Report (AR5; IPCC 2013) concluded with high confidence that, by the end of the twenty-first century, the frequency of daily precipitation extremes will likely increase for midlatitude land and wet tropical regions due to global warming (see also Kharin et al. 2007, 2013; Sillmann et al. 2013a,b; Wuebbles et al. 2014).

These results are further supported by high-resolution regional climate models (RCMs), which brought significant improvements in the representation in both daily and subdaily precipitation extremes (Prein et al. 2013; Tripathi and Dominguez 2013) at the local and regional scale (Maraun et al. 2010). RCMs with a spatial resolution of ~ 10 km using parameterized convection have been shown to adequately capture the intensity of daily precipitation extreme events (Ban et al. 2014). However, a resolution on the order of a few kilometers is required to adequately resolve the convective processes

directly linked to subdaily summer extreme rainfall which occurs at very small scales (Chan et al. 2014; Kendon et al. 2017; Prein et al. 2015; Westra et al. 2014). Convective permitting scales have also clearly improved the model performance in terms of reproducing precipitation circulation with orography (Rasmussen et al. 2011). Convective precipitation may also be very sensitive to the selection of the model physics (Mooney et al. 2017).

Multimodel ensembles of RCM simulations, combining various RCMs and GCMs, were recently produced to assess the impact of climate change over specific regional domains and to assess the impact of regional and global model uncertainties on projections. Examples of such ensembles are the Coordinated Regional Climate Downscaling Experiment (CORDEX) for North America (NA-CORDEX; Mearns et al. 2017) and the North American Regional Climate Change Assessment Program (NARCCAP; Mearns et al. 2012) ensembles for North America and the ENSEMBLES (van der Linden and Mitchell 2009) and EURO-CORDEX (Jacob et al. 2014) ensembles for Europe. However, few studies have investigated changes in more extreme precipitation events over North America (e.g., Mailhot et al. 2007, 2012; Mladjic et al. 2011; Wehner 2013; Zhu 2013) and Europe (e.g., Aalbers et al. 2018; Hosseinzadehtalaei et al. 2018; Rajczak and Schär 2017). In general, large projected changes (mostly increases) have been reported by these studies.

An important issue, relevant to all studies using output from climate models, is the impact of the spatio-temporal resolution on simulated extreme precipitation series. A coarser spatial resolution is expected to smooth out extreme and provide an inaccurate representation of the finescale processes involved in the generation of extreme and spatially heterogeneous extreme precipitation (Chen and Knutson 2008; Volosciuk et al. 2015). These limitations should be kept in mind as it is expected that short-duration extreme precipitation should be more impacted by climate change (see, e.g., Mailhot et al. 2012; Prein et al. 2017; Westra et al. 2014). These spatiotemporal scaling issues have been previously explored with both observational datasets (Gehne et al. 2016; Westra et al. 2014; Zolina et al. 2014) as well as climate model experiments (Chan et al. 2014; Chen and Knutson 2008; Mailhot et al. 2012; Volosciuk et al. 2015) but remain a limitation for most studies.

Large ensembles (LE) are generated by running a climate model many times with slightly different initial conditions, resulting in different simulations for the same time period and forcing scenario after merely a few weeks (Deser et al. 2012a; Martel et al. 2018). LE helps disentangle intermodel variability from natural climate

variability (Fischer et al. 2013; Kay et al. 2015; Martel et al. 2018) and provide climatological series long enough to robustly assess possible changes in very rare events (such as the 100-yr return period event).

These ensembles have gained in popularity over the past years (e.g., Aalbers et al. 2018; Deser et al. 2012a,b, 2014; Fischer et al. 2014; Kay et al. 2015; Martel et al. 2018; Sanderson et al. 2018; Thompson et al. 2015). However, due to their high computational costs, these ensembles are still relatively rare, especially when it comes to high-resolution RCMs (Aalbers et al. 2018; Leduc et al. 2019; Mizuta et al. 2017).

The objectives of this study are twofold: 1) assess the projected future changes in the frequency of large extreme precipitation events (up to 100-yr return period events) using three LE of climate simulations [two global ensembles—Canadian Earth System Model, version 2, Large Ensemble (CanESM2-LE) and Community Earth System Model, version 1, large ensemble (CESM1-LE)—and one regional ensemble—Canadian Regional Climate Model, version 5 (CRCM5-LE)], and 2) check the global consistency of the projected changes in extreme precipitations and evaluate the impact of both the spatial resolution and temporal scale of LE models on the projected future changes. The three LE of climate simulations and the methods used in their production are presented in section 2, while the analysis methods are described in section 3. Results and discussion are shown in section 4. Finally, concluding remarks are presented in section 5.

2. Datasets

Three LE were considered in this study. Two of these ensembles are global, and use two different ESMs, while the third one is produced by an RCM driven by a GCM over two distinct domains.

a. *CanESM2 and CESM1 large ensembles*

The first ensemble is CanESM2-LE from the Canadian Centre for Climate Modeling and Analysis (CCCma), with a 2.8° spatial resolution (Arora et al. 2011; Sigmond and Fyfe 2016; von Salzen et al. 2013). First, five simulations over the 1850–1950 period were launched to obtain five different states of the oceans, and these were then used as the initial conditions for five simulation families. This step allowed accounting for some of the oceanic variability, which is characterized by a much longer response time than the atmosphere. These five initial conditions were each randomly perturbed 10 times, and simulations ran

until 2006 using historical forcing, and then using the representative concentration pathway (RCP) 8.5 forcing scenario (RCP8.5; Meinshausen et al. 2011) until 2100. Fifty simulations (called members) covering the 1950–2100 period, for a total of 7500 (50 simulations \times 150 years) simulated years were therefore produced.

CESM1-LE consists of 40 climate simulations (members) at a 1° resolution covering the 1920–2100 period (Kay et al. 2015). First, a multicentury control simulation starting in 1850, and using constant pre-industrial forcing, was run until 1920. In contrast to CanESM2-LE, all 40 simulations were produced using the same initial ocean state. From there, the air temperature fields were randomly perturbed 40 times at the round-off error level. The RCP8.5 forcing scenario was also introduced from 2006 to the end of the century.

The representation of interannual mean and variability within CanESM2-LE and CESM1-LE was investigated for both the total wet-day precipitation (PRCPTOT; total precipitation on days with precipitation ≥ 1 mm) and the annual maximum 1-day precipitation (RX1day) in a study by Martel et al. (2018). Both precipitation indices were compared against the observed Hadley Centre Global Climate Extremes Index 2 (HadEX2; Donat et al. 2013b; resolution of 2.5° latitude \times 3.75° longitude) and Global Historical Climatology Network-Daily climate extremes (GHCNDEX; Donat et al. 2013a; resolution of 2.5° latitude \times 2.5° longitude) gridded datasets. The spatial patterns of interannual mean and variability were found to be globally in good agreement with those of HadEX2 and GHCNDEX datasets for both PRCPTOT and RX1day, albeit to a lesser extent for the latter.

b. *CRCM5 large ensemble*

CRCM5 (Martynov et al. 2013; Šeparović et al. 2013) was developed by the Université du Québec à Montréal (UQAM) Centre for the Study of Climate Simulations at the Regional Scale [pour l'Étude et la Simulation du Climat à l'Échelle Régionale (ESCER)] in collaboration with ECCC. The CRCM5 was run at a resolution of 0.11° over two different regional domains: northeastern North American (NNA) and European (EU) (Fig. 1). The CRCM5 50-member ensemble (CRCM5-LE; Leduc et al. 2019) was produced within the Climate Change and Hydrological Extremes (ClimEx) project, part of a long-term collaboration between Bavaria and Quebec (<http://www.climex-project.org/>). The 50 members were run using the 6-h atmospheric and daily oceanic field outputs from CanESM2-LE at the boundaries of both domains covering the 1950–2100 period. ClimEx

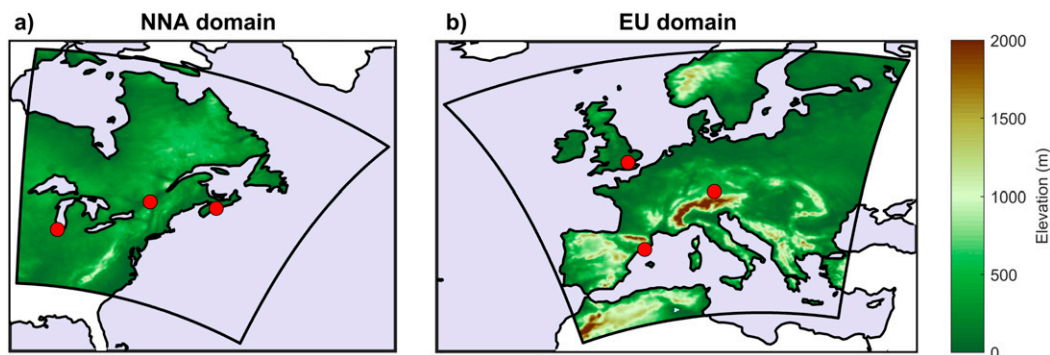


FIG. 1. Digital elevation model (DEM) used in CRCM5-LE for the (a) northeastern North America (NNA) and (b) Europe (EU) domains. Red dots appearing in the NNA domain represent, from left to right, Chicago, Montreal, and Halifax. Red dots appearing in the EU domain correspond, from top to bottom, to London, Munich, and Barcelona.

data will be available for public download in the near future. Six grid points next to large metropolitan areas (three per domain) that will be further analyzed in this study are also shown in Fig. 1. These were selected as results showed that they displayed distinctive pattern of changes of future extreme precipitation.

Evaluation of CRCM5-LE output was performed using different observed gridded datasets for both domains (Leduc et al. 2019). Regarding mean daily precipitation, a wet bias was observed throughout the year for both the NNA and EU domains with a strong dominant component in winter for both domains. A dry bias was also observed in summer for southwestern NNA and eastern Europe. A comparison with a CRCM5 run driven by the ERA-Interim reanalysis (ERA-CRCM5) showed that a significant portion of the wet bias can be attributed to CanESM2-LE (Leduc et al. 2019). The CRCM5 performance, notably in terms of extreme precipitation quantiles and annual and daily cycles, has also been evaluated in a study by Innocenti et al. (2019). A comparison of the ERA-CRCM5 simulation against station records for NNA domain showed good agreement for 2-, 10-, and 25-yr short-duration extreme precipitation quantiles but overestimations for daily and longer-duration extreme precipitation in some regions. The ERA-CRCM5 run provided a good representation of both the annual and diurnal cycles.

3. Methods

Cumulative annual maximum precipitation (AMP) series (AMPS) for various temporal scales (from 1 h to 5 day) were extracted and used to estimate long return periods (i.e., 100-yr return period). Daily and 5-day annual precipitation extremes were first extracted for all grid points of all CanESM2 and CESM1 members

for both the 20-yr reference (1980–99) and future (2080–99) periods. With only hourly outputs being available for CRCM5-LE, moving windows were instead used to extract the AMP (e.g., a 24-h moving window was used instead of the daily value to create the 24-h AMPS). CRCM5-LE 1–120-h (5-day) AMPS were thus similarly constructed for all grid points over both domains. AMPS from the different members were then pooled for each period, leading to a 1000-yr AMPS for CanESM2-LE and CRCM5-LE (20 years \times 50 members) and an 800-yr AMPS for CESM1 (20 years \times 40 members). The framework used in this study is built on the assumption of an ergodic process (Nikiéma et al. 2018), given that the human-induced climate change signal (external forcing) will be dominated by natural variability when investing a short time window (i.e., the time series are stationary over this time window).

Pooling the AMPS from the different members is based on the hypothesis that these series can be considered stationary over the given 20-yr period. The existence of local trends at each grid point for the three LE was therefore assessed using the nonparametric Mann–Kendall test (Kendall 1975) at a 95% confidence level. The distribution of the number of grid points with a given number of members with significant trends was compared to the binomial distributions, and differences between these distributions were assessed through the Kolmogorov–Smirnov test (95% confidence level). The binomial distribution was considered as it represents the distribution of the number of members that would randomly display a significant trend (5% probability to randomly generate significant trends) over 50 trials (members). The null hypothesis was accepted in all cases for both the 1980–99 and 2080–99 periods. Thus, the reference and future 20-yr time series can be considered

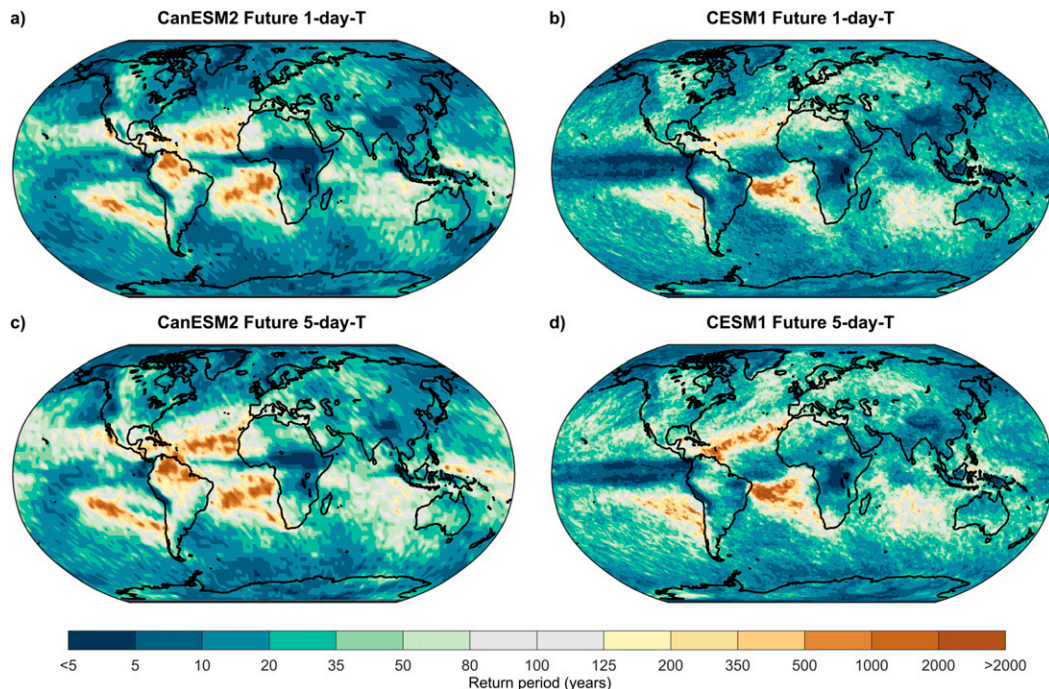


FIG. 2. Maps of the projected return period over the 2080–99 period of the (top) 1- and (bottom) 5-day AMP with same intensity as the 100-yr AMP over the 1980–99 period for (a),(c) CanESM2-LE and (b),(d) CESM1-LE.

stationary. A similar analysis was conducted for 30-yr durations (1980–2009 and 2070–99) and time series for many grid points were found to be not stationary.

The pooled time series were then sorted and used to estimate the empirical quantiles based on the Cunnane plotting position (Cunnane 1978; Meylan et al. 2008). Empirical estimates were used considering the length of available series (1000 years for CanESM2-LE and CRCM5-LE and 800 years for CESM1-LE). The 100-yr return period AMP was first estimated for the reference period at each grid point. The 2080–99 return period corresponding to the 1980–99 100-yr precipitation intensity was then estimated, therefore providing the projected change in the frequency of this extreme event (hereafter, future 1-day-T and 5-day-T for CanESM2-LE and CESM1-LE and future 1-h-T, 24-h-T, and 120-h-T for CRCM5-LE, depending on the temporal scale). A reference 100-yr 24-h rainfall AMP of 100 mm increasing to 130 mm over the future period, and where a 100-mm rainfall now corresponds to a 20-yr AMP can be used as an example. In this case, the future changes in the reference 100-yr AMP could be expressed as a 30% relative increase, or by becoming a 20-yr AMP (an event 5 times as frequent). Expressing the future change in terms of changes in future return period of the reference 100-yr AMP was considered as it gives potential users a sense of the actual severity of the event they may have

experienced in the past (and for which they may have an idea of the impact).

4. Results and discussion

a. Projected changes at the global scale

Projected future changes for 1- and 5-day AMPs at the global scale using CanESM2-LE and CESM1-LE were first analyzed. Figure 2 presents the projected return period over the 2080–99 period of 1- and 5-day AMPs (1-day-T and 5-day-T) having the same intensity as the 100-yr event over the 1980–99 reference period. Cumulative distributions of land gridpoint projected return periods of the reference 100-yr AMP are shown in Fig. 3.

Figure 2 shows that the frequency of future 1-day-T and 5-day-T increase for almost all grid points, with the exception of some subtropical and tropical regions, notably for CanESM2-LE. Previous studies based on the CMIP5 ensemble have shown that these regions have strong natural variability and a relatively low intermodel agreement in the projected changes in precipitation extremes (IPCC 2013; Kharin et al. 2007; Kharin et al. 2013). For instance, both ensembles display opposite signs in the projected changes over the Amazon basin, but CESM1-LE tends to be closer to the results from the CMIP5 intermodel mean obtained in previous studies. Aside from these discrepancies, there is global

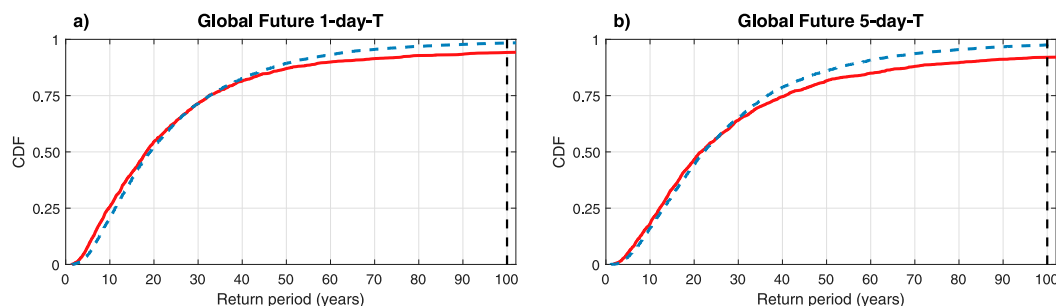


FIG. 3. CDFs of the projected return period over the 2080–99 period of the (a) 1- and (b) 5-day AMP with the same intensity as the 100-yr AMP over the 1980–99 period. Distributions are shown for all land grid points from CanESM2-LE (red curve) and CESM1-LE (blue curve). The dashed vertical line corresponds to the 100-yr return period. Values on the x -axis longer than 100 years are not displayed.

agreement between both large ensembles in the projected global change in precipitation extremes. Global patterns of changes for 1-day-T and 5-day-T for both LE are also very similar (Fig. 2a vs Fig. 2c and Fig. 2b vs Fig. 2d).

Figure 3 shows that there is an overall strong agreement between the distributions of projected changes by CanESM2-LE and CESM1-LE for both 1-day-T and 5-day-T. Approximately 94% (98%) of land grid points for CanESM2-LE and 92% (98%) for CESM1-LE experience more frequent 1-day (5-day) precipitation extremes in the future. The median value of the future 1-day-T (5-day-T) is 18 (22) years for land grid points (without Antarctica) for CanESM2-LE and 19 (22) years for CESM1-LE, meaning that a 100-yr return period over the 1980–99 reference period is about 4–5 times more frequent in 2080–99 for half of the land grid points.

Similar results were obtained for the reference 20-yr AMP both in terms of the sign and the magnitude of the projected changes (Figs. S1 and S2 in the online supplemental material). The median value over land grid points of the future 1-day-T (5-day-T) is 6 (6) years for CanESM2-LE and 6 (7) years CESM1-LE, or between 3 and 4 times more frequent. It should be noted that these results corroborate those obtained in the studies of Kharin et al. (2007, 2013), where the multimodel average (29 CMIP5 models) global median value for all land grid points of the projected return period of the 20-yr daily AMP by 2100 with the same intensity as the 20-yr return period over 1986–2005 was also found to be 6 years.

b. Projected changes over the North American and European domains

The projected return period with the same intensity as the 100-yr AMP over the 1980–99 period simulated by CRCM5-LE over the NNA and EU domains are displayed in Fig. 4. Cumulative distributions of land

gridpoint values at various durations over CRCM5-LE are presented in Fig. 5.

For the NNA domain, an overall increase in frequency of extreme precipitation events is projected (Figs. 4a–c and 5a). A west-to-east gradient toward a greater reduction in the future return period can be seen for all durations, especially for the 1-h AMP. Some orographic effects can be observed for the 1-h AMP as greater reductions in the return period are observed above the Appalachian Mountains (see the topography in Fig. 1a). The shortest projected return periods would be reached over the east coast, with return periods shorter than 10 years for the future 1-h-T, corresponding to more than a tenfold increases in frequency of the reference 100-yr AMP events. Approximately 30% of NNA land grid points experience more than a tenfold increase in the 1-h AMP. This fraction quickly decreases as the duration increases since fewer than 5% of land grid points experience a tenfold increase or greater for the 24-h AMP. For the future 24-h-T, the lower projected return period values would range between 10 and 20 years, representing a five- to tenfold increase in frequency. As shown in Fig. 5a, the median future 1-h-T is 14 years, while for the future 24-h-T and 120-h-T, median values over land grid points are 18 and 20 years, respectively.

Significant increases in precipitation extremes over most of the EU domain were also observed, although these increases are not as high as those seen over the NNA domain (Figs. 4d–f and 5b). For the 1-h AMP (future 1-h-T), the median future return period is 26, as years compared to 35 and 42 years respectively for the 24-h and 120-h AMP. The greatest reductions in return period are observed in high-altitude regions (e.g., the European Alps; also see Giorgi et al. 2016), the Scandinavian countries and Ireland (with values ranging between 5 and 10-yr return periods for the 1-h AMP). It should be noted that the European Alps can easily be seen in Figs. 4d–f, especially for the 1-h duration. Other

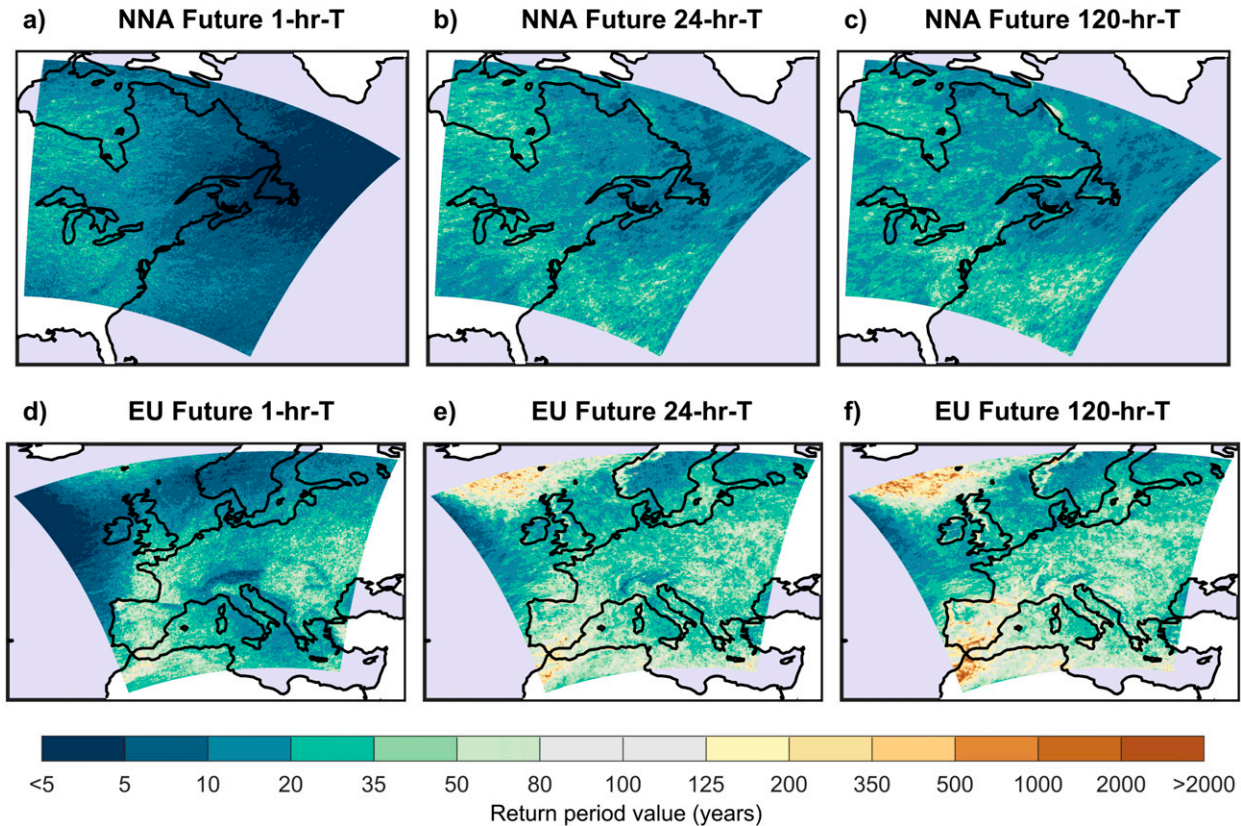


FIG. 4. Projected return period over the 2080–99 future period of the (a),(d) 1-, (b),(e) 24-, and (c),(f) 120-h AMP with same intensity as the 100-yr AMP over the 1980–99 period as simulated by CRCM5-LE for the (top) NNA and (bottom) EU domains.

high-altitude regions also stand out, such as the Pyrenees, the Dinaric Alps, the Balkan Mountains, and the Carpathian Mountains (see Figs. 4d and 1b for high-altitude regions). Figures 5c and 5d also show that projected increases in extreme precipitation at the hourly and subdaily scales are greater than for daily and multiday extremes over both regions.

Results from CRCM5-LE, CanESM2-LE, and CESM1-LE were then compared to assess the consistency of projected changes for 1- and 5-day (24 and 120 h for CRCM5-LE) AMP over the NNA and EU domains. A total of 81 (100) land grid points of CanESM2-LE and 525 (662) for CESM1-LE were therefore considered for the NNA (EU) domains. The CDF of land gridpoint projected return periods over the 2080–99 period for the three LE for both domains are presented in Fig. 6. Maps of the projected changes are shown in Figs. S3 and S4.

Figures 6a–c show that all land grid points of the NNA domain experience increases in AMP (corresponding to decreases in the projected return period) according to the three LE for both 1-day (24 h) and 5-day (120 h) AMP. A very large fraction of land grid points similarly displays large increases in extreme precipitation for the

EU domain [100%, 94%, and 94% for 1-day (24 h) AMP and 95%, 91%, and 86% for 5-day (120 h) AMP according to CanESM2-LE, CESM1-LE, and CRCM5-LE, respectively]. Also, for the NNA domain, all ensembles point to large increases in AMP, with more than four- to fivefold increases in frequency for half of the land grid points. With respect to the EU domain, half of the land grid points display more than two- to threefold increases in frequency of the reference 100-yr AMP. In general, other studies based on different methodologies and on various extreme precipitation metrics have also reported significant increases over the NNA (Mailhot et al. 2007, 2012; Mladjic et al. 2011; Wehner 2013; Wuebbles et al. 2014) and EU (Aalbers et al. 2018; Rajczak and Schär 2017) domains, but in terms of relative changes for the different return periods investigated.

Figure 6 also shows that, on both domains, projected future return periods associated with 1-day (24 h) and 5-day (120 h) 100-yr AMP in the reference climate as simulated by CanESM2-LE are shorter than corresponding values simulated by CESM1-LE and CRCM5-LE. It should be noted that despite large differences in terms of

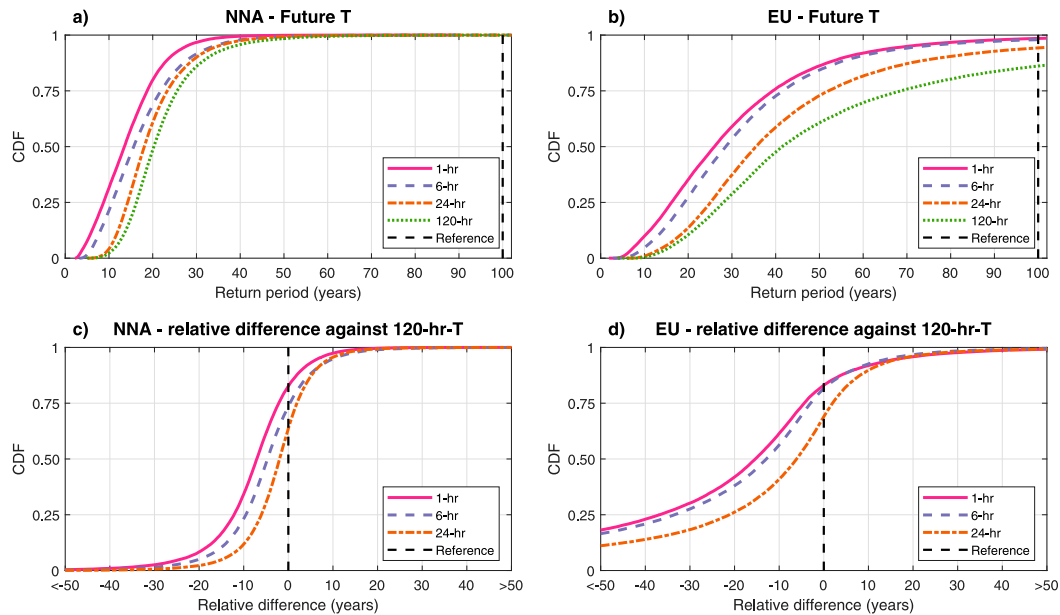


FIG. 5. CDFs of the projected return period over the 2080–99 period of AMP with the same intensity as the 100-yr AMP over the 1980–99 period for (a),(b) durations ranging from 1 to 120 h and (c),(d) the differences between grid point 120-h-T values and corresponding 1-h-T (pink), 6-h-T (blue), and 24-h-T (orange) values. Only land grid points inside the (left) NNA domain and (right) EU domain were considered. The dashed vertical line corresponds to the 100-yr return period. Values on the x axis longer than 100 years are not displayed in (a) and (b) and those smaller than 50 years are not displayed in (c) and (d).

spatial resolution and model structures, projected changes are consistent across all three climate models on both domains for the 100-yr return period AMP. It is also interesting to note that, when projected changes are expressed in terms of changes in return period, the greatest changes in future 100-yr return period AMP are estimated by CanESM2-LE, which has the coarsest spatial scale.

Figure 7 presents the CDF of the land gridpoint relative changes (1 day/24 h and 5 day/120 h) occurring between the 1980–99 and 2080–99 periods for 20- and 100-yr AMP over both domains. This figure provides a complementary perspective to Fig. 6. It shows the projected future increases in terms of AMP intensity of the reference 100-yr AMP, while Fig. 6 shows changes in terms of frequency. Complementary maps of relative changes in the 20- and 100-yr AMP for Fig. 7 are shown in Figs. S5–S8.

Figure 7 shows consistent results over the NNA domain with all ensembles projecting similar increases for both 20- and 100-yr as well as 1-day (24 h) and 5-day (120 h) AMP. For instance, all three ensembles project that a larger proportion of land grid points experience greater increases for 100-yr AMP than for 20-yr AMP, and greater increases for 1-day (24 h) AMP than for 5-day (120 h) AMP. These are important results, as they suggest that climate change impact more extreme events (associated with long return periods), more

severely, and have a more severe impact on daily AMP than on multiday AMP [result also reported by Pendergrass (2018)]. Similar results can also be observed over the EU domain (Figs. 7b–d). Increases in that case are lower (with up to a quarter of the land grid points experiencing relative decreases), but still greater for longer return periods and daily AMP (see also Figs. S5 and S6 for the 20-yr AMP, Figs. S7 and S8 for the 100-yr AMP). The picture over both domains is remarkably consistent for all three LE and for both durations (1 day/24 h and 5 day/120 h).

A comparison of gridpoint values from the three ensembles over the reference period (1980–99; Figs. S9–S14) shows that AMP values as simulated by CRCM5-LE are much greater than corresponding values estimated from CESM1-LE or CanESM2-LE for all durations, return periods, and domains. Considering that the output from the different climate models are interpreted as spatial average over each grid point, the spatial resolution can partly explain these differences in AMP values (Chen and Knutson 2008; Sunyer et al. 2013), especially for 100-yr return period AMP. Increasing the spatial resolution enables a better representation of local precipitation extremes, notably for summer convective storms (Maraun et al. 2010; Prein et al. 2013; Tripathi and Dominguez 2013). It is, however, interesting to note that, despite these large

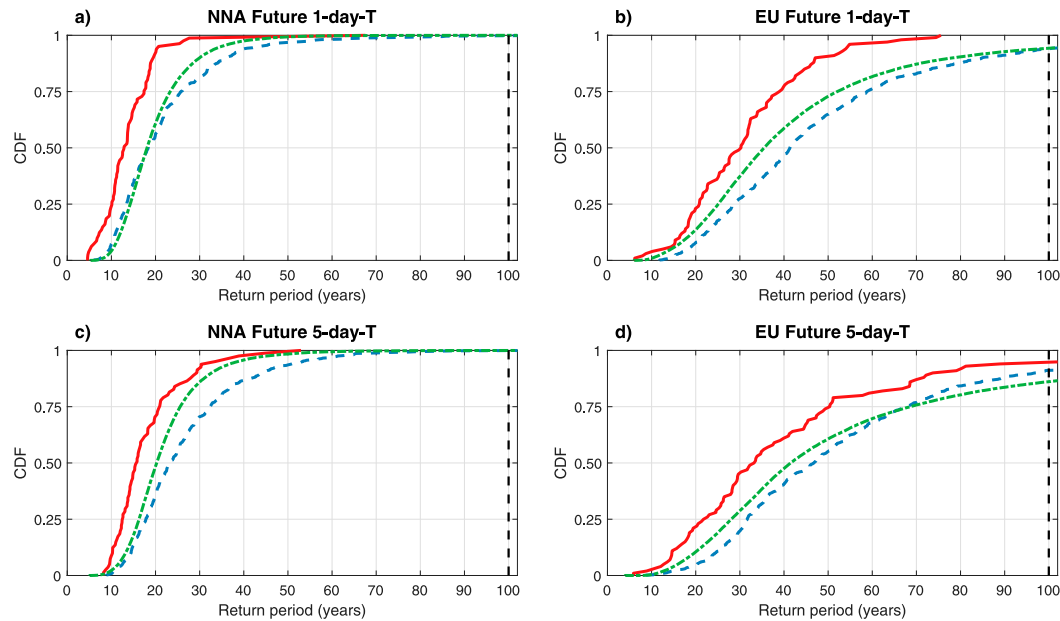


FIG. 6. CDFs of the projected return period over the 2080–99 period for (a),(b) 1-day (24 h) and (c),(d) 5-day (120 h) AMP for CanESM2-LE and CESM1-LE (CRCM5-LE) with the same intensity as the 100-yr AMP over the 1980–99 period. Only land grid points from CanESM2-LE (red), CESM1-LE (blue), and CRCM5-LE (green) over the (left) NNA and (right) EU domains were considered. The dashed vertical lines correspond to the 100-yr return period. Values on the x-axis longer than 100 years are not shown.

differences in terms of simulated AMP quantiles in the reference climate, the three ensembles provide quite consistent changes in terms of daily and multiday AMP increases over both domains.

c. Projected changes for specific grid points close to large urbanized areas

Considering the importance of assessing the impact of climate changes on subdaily extreme precipitation in urban areas, grid points corresponding to six cities, three located in the NNA (Chicago, Illinois; Halifax, Nova Scotia, Canada; Montreal, Quebec, Canada) and three in the EU (Barcelona, Spain; London, United Kingdom; Munich, Germany) domains were selected (Fig. 1). Projected relative changes occurring between the 1980–99 and 2080–99 periods for AMP durations from 1 to 120 h and return periods equal to 2, 20, and 100 years were assessed using CRCM5-LE (Fig. 8). Bootstrapping with resampling (10 000 samples) was used to estimate the 95% confidence interval. This was done by computing the relative change between both periods (1980–99 and 2080–99) confidence intervals.

Relative changes curves shown in Fig. 8 point to large increases for all city grid points, durations, and frequencies (except for the Barcelona grid point for the short return period and long-duration AMP and for London grid point where relative changes are almost

identical for the three return periods), reaching up to a 71% increase for Halifax grid point. However, while large relative increases are observed, they differ strongly for each duration and frequency analyzed. In general, the relative increases tend to be larger as the return period increases or as the duration decreases. Furthermore, there are strong local variations among the city grid points.

It should be noted that increases in AMP relative changes as durations decrease are not as smooth for the 100-yr return period (e.g., for the Chicago grid point, relative increases for the 6-h 100-yr AMP are less than for 3- and 1-h AMP increases). This may be due to larger uncertainties (sampling errors) on empirical AMP quantile estimates in this case. These can be significant, even when 1000-yr series are used to empirically estimate the 100-yr AMP.

Although these projected relative changes are based on a single land gridpoint series (some regional analyses could provide a more regional picture and reduce sampling uncertainties for the 100-yr AMP), they show that large increases in AMP can be expected at local scales and should be accounted for, even if these estimates remain uncertain.

5. Concluding remarks

The three large ensembles (LE) of climate simulations, two global (the 40-member CESM1-LE and the

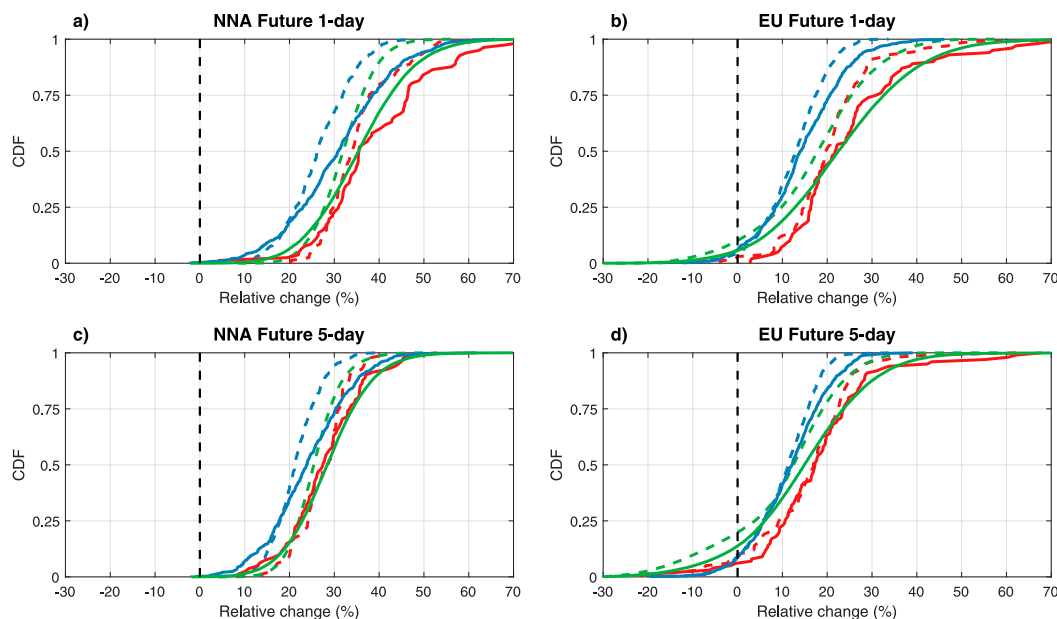


FIG. 7. CDFs of the projected relative changes (%) in the 20-yr (dashed curves) and 100-yr (continuous curves) AMP between the 1980–99 and the 2080–99 period for (a), (b) 1-day (24 h) and (c), (d) 5-day (120 h) AMP for CanESM2-LE and CESM1-LE (CRCM5-LE) over the (left) NNA and (right) EU domains. Distributions are shown for CanESM2-LE (red), CESM1-LE (blue), and CRCM5-LE (green) land grid points.

50-member CanESM2-LE), and one based on a regional model (the 50-member CRCM5-LE), were considered in this study. CRCM5-LE simulations are available over two domains, covering northeastern North America (NNA) and the other one covering Europe (EU). The CRCM5-LE regional ensemble was generated by dynamically downscaling the CanESM2-LE over the 1950–2100 period. The RCP8.5 forcing scenario was considered for all three ensembles.

The three ensembles point to a significant reduction in the projected return period (corresponding to an increase in intensity) over the 2080–99 period of the 100-yr AMP over the 1980–2000 period at both global and regional scales. The 100-yr annual maximum precipitation (AMP) is more frequent in future climates for most land grid points, with up to a tenfold frequency increase for some grid points. Over a given state or country, this means that larger populations and more cities, towns, and municipalities will face larger extreme rainfall events.

Future return periods of 100-yr 1-day and 5-day AMP estimated from CanESM2-LE and CESM1-LE are consistent over most of the land grid points, aside from some discrepancies over subtropical and tropical regions. At the regional level, on the northeastern North America and Europe domains, CRCM5-LE also showed similar changes in future return periods for durations ranging from 1 to 120 h.

More specifically, at the global scale using both CanESM2-LE and CESM1-LE, 100-yr 1-day and 5-day AMP over the reference period become 4–5 times more frequent by the end of this century for half of the world’s land grid points. At the regional scale, all three LE project major increase in the 100-yr 1- and 5-day (24 and 120 h for CRCM5-LE) AMP, with more than half of land NNA (EU) grid points experiencing a four- to fivefold (two- to threefold) increase in frequency. Despite having different model structures and resolutions, all three ensembles point to a strong reduction in the projected return period of the reference 100-yr AMP for the 1- and 5-day durations.

Results suggest that complex orography plays an important role in the projected changes. Greater reductions in return periods for high-altitude regions are observed within the regional model (e.g., the Appalachian Mountains in the NNA domain and the Alps in the Europe domain), notably for the 1-h AMP. Similar results, showing that complex topography has an impact on future extreme precipitations, have also been reported by Ban et al. (2015) and Prein et al. (2017). This shows the “added value” of higher spatial resolution when assessing regional changes in extreme precipitation. The impact of complex topography on the projected changes in precipitation extremes should be further investigated in future work.

Looking more specifically at the impact of AMP durations on projected changes for the regional CRCM5-LE, it was shown that short-duration 100-yr AMP experiences

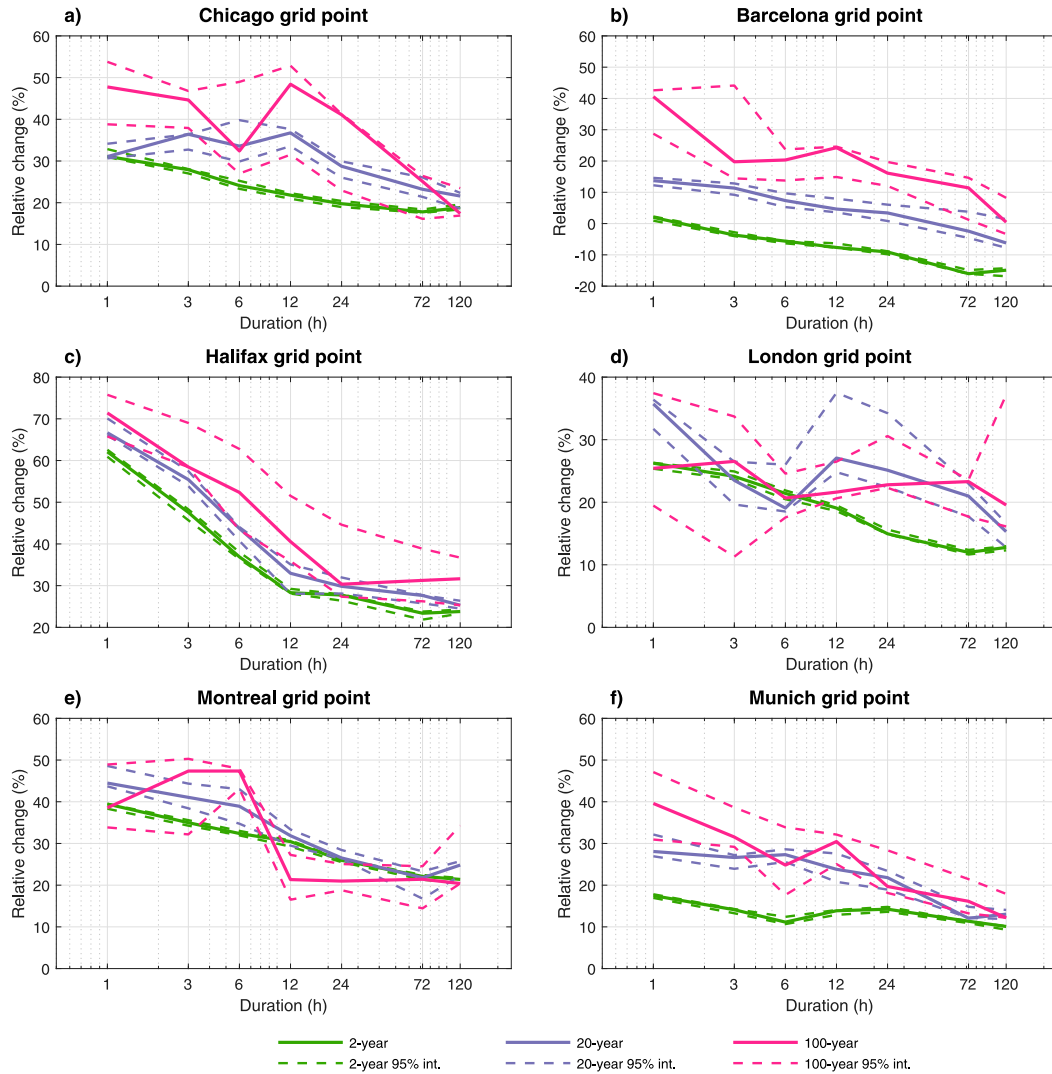


FIG. 8. Relative change (%) in AMP intensity between the 1980–99 and 2080–99 periods as a function of duration for grid points including: (a) Chicago, (b) Barcelona, (c) Halifax, (d) London, (e) Montreal, and (f) Munich as estimated from CRCM5-LE. Two-year (green), 20-yr (blue) and 100-yr (pink) return period AMP are shown. The dashed curves show the 95% empirical confidence intervals.

longer return period reductions. Therefore, the model results imply that the impact of climate changes are greater on short-duration AMP.

Looking at the relative changes curves at some specific sites, it was shown that higher relative increases can be expected for shorter durations and longer return periods with strong local variations (from city to city). For example, projected increases in intensity/frequency of the 1-h 100-yr rainfall are greater than for the 6-h 20-yr rainfall. These results suggest that, in order to take into consideration the projected changes in extreme precipitation in actual design of hydraulic infrastructure, different increases should be considered depending on duration, return periods, and regions.

These large increases in the frequency of extreme precipitation events have important implications since the design of many types of infrastructure relies on estimations of extreme precipitation for various durations and return periods. Based on the results highlighted in this work (which corroborate those from other recent studies), climate change adaptation strategies and design criteria must be revised to account for these expected large reductions in the projected future return periods for precipitation extremes.

Several limitations of this study should be investigated in future work. A single regional model was used to explore the subdaily time scale. There are, however, very few examples of such large ensembles run at the

regional scale (Aalbers et al. 2018; Mizuta et al. 2017). Analyses combining many LE generated from various RCM–GCM combinations should help in assessing the impact of climate model structure and resolution on projected subdaily extreme precipitation. Multimodel analysis is important since it is expected that intermodel variability is likely one of the main sources of uncertainties for long-term projections of extreme precipitation. Initiatives such as the High Resolution Model Intercomparison Project (HighResMIP; Haarsma et al. 2016) could provide the necessary datasets to further investigate this source of uncertainty.

Despite CRCM5's relatively high spatial resolution (0.11°), many processes, such as deep convection, occur at spatial scales too small to be resolved explicitly at the model grid scale, and are therefore parameterized. While synoptic weather patterns are generally well simulated at this resolution, a finer resolution is required to comprehensively simulate small scale convective events (Chan et al. 2014; Kendon et al. 2017; Prein et al. 2017, 2015). Convective-permitting models (CPM) are therefore needed to resolve subdaily convective extreme precipitation events, and confirm the results obtained from convection-parameterized regional models for subdaily extreme precipitation (Prein et al. 2015). It should be noted that there are new efforts to generate multimodel ensembles at the convective-permitting scales (Coppola et al. 2019; Prein et al. 2015).

Only the RCP8.5 forcing scenario, which is a high-end emission scenario (IPCC 2013; Meinshausen et al. 2011), was considered in this study. Clearly, other forcing scenarios (e.g., RCP2.6 or RCP4.5) should be considered in order to assess the sensitivity of the projected changes to anthropogenic forcing. This is even more important as emission scenarios play an important role for the more distant future periods, as considered in this work. Some authors suggest that the most likely future emission scenario is probably closer to the middle range of forcing scenarios currently proposed, such as RCP4.5 or RCP6.0 (Raftery et al. 2017).

Acknowledgments. This work was partly financed through the ClimEx project funded by the Bavarian State Ministry for the Environment and Consumer Protection. The authors acknowledge the contributions from the Canadian Centre for Climate Modelling and Analysis [Environment and Climate Change Canada (ECCC)] for simulating and making available the CanESM2-LE used in this study, and the Canadian Sea Ice and Snow Evolution Network for proposing the simulations. The authors would also like to thank the Ouranos Consortium for helping with data transfer. The CanESM2-LE dataset is now available on the ECCC website (<http://collaboration.cmc.ec.gc.ca/cmc/ccma/CanSISE/output/CCCma/CanESM2/>). The CESM1

ensemble was downloaded from the Large Ensemble Community Project (LENS) website (<http://www.cesm.ucar.edu/projects/community-projects/LENS/>). The CRCM5 was developed by the ESCER Centre at Université du Québec à Montréal (UQAM; www.escer.uqam.ca) in collaboration with ECCC. Computations with the CRCM5 for the ClimEx project were made on the SuperMUC supercomputer at the Leibniz Supercomputing Centre (LRZ) of the Bavarian Academy of Sciences and Humanities. The operation of this supercomputer is funded via the Gauss Centre for Supercomputing (GCS) by the German Federal Ministry of Education and Research and the Bavarian State Ministry of Education, Science and the Arts.

REFERENCES

- Aalbers, E., G. Lenderink, E. van Meijgaard, and B. J. J. M. van den Hurk, 2018: Local-scale changes in mean and heavy precipitation in Western Europe, climate change or internal variability? *Climate Dyn.*, **50**, 4745–4766, <https://doi.org/10.1007/s00382-017-3901-9>.
- Alexander, L. V., and Coauthors, 2006: Global observed changes in daily climate extremes of temperature and precipitation. *J. Geophys. Res.*, **111**, D05109, <https://doi.org/10.1029/2005JD006290>.
- Arnone, E., D. Pumo, F. Viola, L. V. Noto, and G. La Loggia, 2013: Rainfall statistics changes in Sicily. *Hydrol. Earth Syst. Sci.*, **17**, 2449–2458, <https://doi.org/10.5194/hess-17-2449-2013>.
- Arora, V. K., and Coauthors, 2011: Carbon emission limits required to satisfy future representative concentration pathways of greenhouse gases. *Geophys. Res. Lett.*, **38**, <https://doi.org/10.1029/2010GL046270>.
- Ban, N., J. Schmidli, and C. Schär, 2014: Evaluation of the convection-resolving regional climate modeling approach in decade-long simulations. *J. Geophys. Res.*, **119**, 7889–7907, <https://doi.org/10.1002/2014JD021478>.
- , —, and —, 2015: Heavy precipitation in a changing climate: Does short-term summer precipitation increase faster? *Geophys. Res. Lett.*, **42**, 1165–1172, <https://doi.org/10.1002/2014GL062588>.
- Brommer, D. M., R. S. Cerveny, and R. C. Balling, 2007: Characteristics of long-duration precipitation events across the United States. *Geophys. Res. Lett.*, **34**, L22712, <https://doi.org/10.1029/2007GL031808>.
- Burn, D. H., R. Mansour, K. Zhang, and P. H. Whitfield, 2011: Trends and variability in extreme rainfall events in British Columbia. *Can. Water Resour. J.*, **36**, 67–82, <https://doi.org/10.4296/cwrj3601067>.
- Chan, S. C., E. J. Kendon, H. J. Fowler, S. Blenkinsop, N. M. Roberts, and C. A. T. Ferro, 2014: The value of high-resolution Met Office regional climate models in the simulation of multihourly precipitation extremes. *J. Climate*, **27**, 6155–6174, <https://doi.org/10.1175/JCLI-D-13-00723.1>.
- Chen, C.-T., and T. Knutson, 2008: On the verification and comparison of extreme rainfall indices from climate models. *J. Climate*, **21**, 1605–1621, <https://doi.org/10.1175/2007JCLI1494.1>.
- Coppola, E., and Coauthors, 2019: A first-of-its-kind multi-model convection permitting ensemble for investigating convective phenomena over Europe and the Mediterranean. *Climate Dyn.*, <https://doi.org/10.1007/s00382-018-4521-8>, in press.

- Cunnane, C., 1978: Unbiased plotting positions—A review. *J. Hydrol.*, **37**, 205–222, [https://doi.org/10.1016/0022-1694\(78\)90017-3](https://doi.org/10.1016/0022-1694(78)90017-3).
- Deser, C., R. Knutti, S. Solomon, and A. S. Phillips, 2012a: Communication of the role of natural variability in future North American climate. *Nat. Climate Change*, **2**, 775–779, <https://doi.org/10.1038/nclimate1562>.
- , A. Phillips, V. Bourdette, and H. Teng, 2012b: Uncertainty in climate change projections: The role of internal variability. *Climate Dyn.*, **38**, 527–546, <https://doi.org/10.1007/s00382-010-0977-x>.
- , —, M. A. Alexander, and B. V. Smoliak, 2014: Projecting North American climate over the next 50 years: Uncertainty due to internal variability. *J. Climate*, **27**, 2271–2296, <https://doi.org/10.1175/JCLI-D-13-00451.1>.
- Donat, M. G., L. V. Alexander, H. Yang, I. Durre, R. Vose, and J. Caesar, 2013a: Global land-based datasets for monitoring climatic extremes. *Bull. Amer. Meteor. Soc.*, **94**, 997–1006, <https://doi.org/10.1175/BAMS-D-12-00109.1>.
- , and Coauthors, 2013b: Updated analyses of temperature and precipitation extreme indices since the beginning of the twentieth century: The HadEX2 dataset. *J. Geophys. Res.*, **118**, 2098–2118, <https://doi.org/10.1002/jgrd.50150>.
- Easterling, D. R., J. L. Evans, P. Y. Groisman, T. R. Karl, K. E. Kunkel, and P. Ambenje, 2000: Observed variability and trends in extreme climate events: A brief review. *Bull. Amer. Meteor. Soc.*, **81**, 417–425, [https://doi.org/10.1175/1520-0477\(2000\)081<0417:OVATIE>2.3.CO;2](https://doi.org/10.1175/1520-0477(2000)081<0417:OVATIE>2.3.CO;2).
- Fischer, E. M., U. Beyerle, and R. Knutti, 2013: Robust spatially aggregated projections of climate extremes. *Nat. Climate Change*, **3**, 1033–1038, <https://doi.org/10.1038/nclimate2051>.
- , J. Sedláček, E. Hawkins, and R. Knutti, 2014: Models agree on forced response pattern of precipitation and temperature extremes. *Geophys. Res. Lett.*, **41**, 8554–8562, <https://doi.org/10.1002/2014GL062018>.
- Gehne, M., T. M. Hamill, G. N. Kiladis, and K. E. Trenberth, 2016: Comparison of global precipitation estimates across a range of temporal and spatial scales. *J. Climate*, **29**, 7773–7795, <https://doi.org/10.1175/JCLI-D-15-0618.1>.
- Giorgi, F., C. Torma, E. Coppola, N. Ban, C. Schär, and S. Somot, 2016: Enhanced summer convective rainfall at Alpine high elevations in response to climate warming. *Nat. Geosci.*, **9**, 584–589, <https://doi.org/10.1038/ngeo2761>.
- Groisman, P. Ya., R. W. Knight, D. R. Easterling, T. R. Karl, G. C. Hegerl, and V. N. Razuvaev, 2005: Trends in intense precipitation in the climate record. *J. Climate*, **18**, 1326–1350, <https://doi.org/10.1175/JCLI3339.1>.
- Haarsma, R. J., and Coauthors, 2016: High Resolution Model Intercomparison Project (HighResMIP v1.0) for CMIP6. *Geosci. Model Dev.*, **9**, 4185–4208, <https://doi.org/10.5194/gmd-9-4185-2016>.
- Hosseinzadehtalaei, P., H. Tabari, and P. Willems, 2018: Precipitation intensity–duration–frequency curves for central Belgium with an ensemble of EURO-CORDEX simulations, and associated uncertainties. *Atmos. Res.*, **200**, 1–12, <https://doi.org/10.1016/j.atmosres.2017.09.015>.
- Innocenti, S., A. Mailhot, A. Frigon, A. J. Cannon, and M. Leduc, 2019: Observed and simulated precipitation over northeast North America: How do subdaily extremes scale in space and time? *J. Climate*, in press.
- IPCC, 2013: *Climate Change 2013: The Physical Science Basis*. Cambridge University Press, 1535 pp., <https://doi.org/10.1017/CBO9781107415324>.
- Jacob, D., and Coauthors, 2014: EURO-CORDEX: New high-resolution climate change projections for European impact research. *Reg. Environ. Change*, **14**, 563–578, <https://doi.org/10.1007/s10113-013-0499-2>.
- Katz, R. W., 2013: Statistical methods for nonstationary extremes. *Extremes in a Changing Climate: Detection, Analysis and Uncertainty*, Springer, 15–37.
- Kay, J. E., and Coauthors, 2015: The Community Earth System Model (CESM) Large Ensemble project: A community resource for studying climate change in the presence of internal climate variability. *Bull. Amer. Meteor. Soc.*, **96**, 1333–1349, <https://doi.org/10.1175/BAMS-D-13-00255.1>.
- Kendall, M. G., 1975: *Rank Correlation Methods*. 4th ed. Charles Griffin, 202 pp.
- Kendon, E. J., and Coauthors, 2017: Do convection-permitting regional climate models improve projections of future precipitation change? *Bull. Amer. Meteor. Soc.*, **98**, 79–93, <https://doi.org/10.1175/BAMS-D-15-0004.1>.
- Kharin, V. V., F. W. Zwiers, X. Zhang, and G. C. Hegerl, 2007: Changes in temperature and precipitation extremes in the IPCC ensemble of global coupled model simulations. *J. Climate*, **20**, 1419–1444, <https://doi.org/10.1175/JCLI4066.1>.
- , —, —, and M. Wehner, 2013: Changes in temperature and precipitation extremes in the CMIP5 ensemble. *Climatic Change*, **119**, 345–357, <https://doi.org/10.1007/s10584-013-0705-8>.
- Kunkel, K. E., and Coauthors, 2013: Monitoring and understanding trends in extreme storms: State of knowledge. *Bull. Amer. Meteor. Soc.*, **94**, 499–514, <https://doi.org/10.1175/BAMS-D-11-00262.1>.
- Leahy, P. G., and G. Kiely, 2011: Short duration rainfall extremes in Ireland: Influence of climatic variability. *Water Resour. Manage.*, **25**, 987–1003, <https://doi.org/10.1007/s11269-010-9737-2>.
- Leduc, M., and Coauthors, 2019: ClimEx project: A 50-member ensemble of climate change projections at 12-km resolution over Europe and northeastern North America with the Canadian Regional Climate Model (CRCM5). *J. Appl. Meteor. Climatol.*, **58**, 663–693, <https://doi.org/10.1175/JAMC-D-18-0021.1>.
- Lenderink, G., and H. J. Fowler, 2017: Understanding rainfall extremes. *Nat. Climate Change*, **7**, 391, <https://doi.org/10.1038/nclimate3305>.
- , H. Y. Mok, T. C. Lee, and G. J. van Oldenborgh, 2011: Scaling and trends of hourly precipitation extremes in two different climate zones—Hong Kong and the Netherlands. *Hydrol. Earth Syst. Sci.*, **15**, 3033–3041, <https://doi.org/10.5194/hess-15-3033-2011>.
- Madsen, H., K. Arnbjerg-Nielsen, and P. S. Mikkelsen, 2009: Update of regional intensity–duration–frequency curves in Denmark: Tendency towards increased storm intensities. *Atmos. Res.*, **92**, 343–349, <https://doi.org/10.1016/j.atmosres.2009.01.013>.
- , D. Lawrence, M. Lang, M. Martinkova, and T. R. Kjeldsen, 2014: Review of trend analysis and climate change projections of extreme precipitation and floods in Europe. *J. Hydrol.*, **519**, 3634–3650, <https://doi.org/10.1016/j.jhydrol.2014.11.003>.
- Mailhot, A., and S. Duchesne, 2010: Design criteria of urban drainage infrastructures under climate change. *J. Water Resour. Plann. Manage.*, **136**, 201–208, [https://doi.org/10.1061/\(ASCE\)WR.1943-5452.0000023](https://doi.org/10.1061/(ASCE)WR.1943-5452.0000023).
- , —, D. Caya, and G. Talbot, 2007: Assessment of future change in intensity–duration–frequency (IDF) curves for southern Quebec using the Canadian Regional Climate Model (CRCM). *J. Hydrol.*, **347**, 197–210, <https://doi.org/10.1016/j.jhydrol.2007.09.019>.
- , I. Beauregard, G. Talbot, D. Caya, and S. Biner, 2012: Future changes in intense precipitation over Canada assessed from multi-model NARCCAP ensemble simulations. *Int. J. Climatol.*, **32**, 1151–1163, <https://doi.org/10.1002/joc.2343>.

- Maraun, D., and Coauthors, 2010: Precipitation downscaling under climate change: Recent developments to bridge the gap between dynamical models and the end user. *Rev. Geophys.*, **48**, RG3003, <https://doi.org/10.1029/2009RG000314>.
- Martel, J.-L., A. Mailhot, F. Brissette, and D. Caya, 2018: Role of natural climate variability in the detection of anthropogenic climate change signal for mean and extreme precipitation at local and regional scales. *J. Climate*, **31**, 4241–4263, <https://doi.org/10.1175/JCLI-D-17-0282.1>.
- Martynov, A., R. Laprise, L. Sushama, K. Winger, L. Šeparović, and B. Dugas, 2013: Reanalysis-driven climate simulation over CORDEX North America domain using the Canadian Regional Climate Model, version 5: Model performance evaluation. *Climate Dyn.*, **41**, 2973–3005, <https://doi.org/10.1007/s00382-013-1778-9>.
- Mearns, L. O., and Coauthors, 2012: The North American Regional Climate Change Assessment Program: Overview of phase I results. *Bull. Amer. Meteor. Soc.*, **93**, 1337–1362, <https://doi.org/10.1175/BAMS-D-11-00223.1>.
- , S. McGinnis, D. Korytina, R. Arritt, S. Biner, and M. Bukovsky, 2017: The NA-CORDEX dataset, version 1.0. NCAR Climate Data Gateway, accessed 18 February 2019, <https://doi.org/10.5065/D6SJ1JCH>.
- Meinshausen, M., and Coauthors, 2011: The RCP greenhouse gas concentrations and their extensions from 1765 to 2300. *Climatic Change*, **109**, 213, <https://doi.org/10.1007/s10584-011-0156-z>.
- Meylan, P., A.-C. Favre, and A. Musy, 2008: *Hydrologie Fréquentielle: Une Science Prédictive*. PPUR Presses Polytechniques, 173 pp.
- Milly, P. C. D., J. Betancourt, M. Falkenmark, R. M. Hirsch, Z. W. Kundzewicz, D. P. Lettenmaier, and R. J. Stouffer, 2008: Stationarity is dead: Whither water management? *Science*, **319**, 573–574, <https://doi.org/10.1126/science.1151915>.
- Min, S.-K., X. Zhang, F. W. Zwiers, and G. C. Hegerl, 2011: Human contribution to more-intense precipitation extremes. *Nature*, **470**, 378–381, <https://doi.org/10.1038/nature09763>.
- Mizuta, R., and Coauthors, 2017: Over 5,000 years of ensemble future climate simulations by 60-km global and 20-km regional atmospheric models. *Bull. Amer. Meteor. Soc.*, **98**, 1383–1398, <https://doi.org/10.1175/BAMS-D-16-0099.1>.
- Mladjic, B., L. Sushama, M. N. Khaliq, R. Laprise, D. Caya, and R. Roy, 2011: Canadian RCM projected changes to extreme precipitation characteristics over Canada. *J. Climate*, **24**, 2565–2584, <https://doi.org/10.1175/2010JCLI3937.1>.
- Mooney, P. A., C. Broderick, C. L. Bruyère, F. J. Mulligan, and A. F. Prein, 2017: Clustering of observed diurnal cycles of precipitation over the United States for evaluation of a WRF multiphysics regional climate ensemble. *J. Climate*, **30**, 9267–9286, <https://doi.org/10.1175/JCLI-D-16-0851.1>.
- Muschinski, T., and J. I. Katz, 2013: Trends in hourly rainfall statistics in the United States under a warming climate. *Nat. Climate Change*, **3**, 577, <https://doi.org/10.1038/nclimate1828>.
- Nikiéma, O., R. Laprise, and B. Dugas, 2018: Energetics of transient-eddy and inter-member variabilities in global and regional climate model simulations. *Climate Dyn.*, **51**, 249–268, <https://doi.org/10.1007/s00382-017-3918-0>.
- Ntegeka, V., and P. Willems, 2008: Trends and multidecadal oscillations in rainfall extremes, based on a more than 100-year time series of 10 min rainfall intensities at Uccle, Belgium. *Water Resour. Res.*, **44**, W07402, <https://doi.org/10.1029/2007WR006471>.
- Pendergrass, A. G., 2018: What precipitation is extreme? *Science*, **360**, 1072–1073, <https://doi.org/10.1126/science.aat1871>.
- Prein, A. F., G. J. Holland, R. M. Rasmussen, J. Done, K. Ikeda, M. P. Clark, and C. H. Liu, 2013: Importance of regional climate model grid spacing for the simulation of heavy precipitation in the Colorado headwaters. *J. Climate*, **26**, 4848–4857, <https://doi.org/10.1175/JCLI-D-12-00727.1>.
- , and Coauthors, 2015: A review on regional convection-permitting climate modeling: Demonstrations, prospects, and challenges. *Rev. Geophys.*, **53**, 323–361, <https://doi.org/10.1002/2014RG000475>.
- , R. M. Rasmussen, K. Ikeda, C. Liu, M. P. Clark, and G. J. Holland, 2017: The future intensification of hourly precipitation extremes. *Nat. Climate Change*, **7**, 48–52, <https://doi.org/10.1038/nclimate3168>.
- Raftery, A. E., A. Zimmer, D. M. W. Frierson, R. Startz, and P. Liu, 2017: Less than 2°C warming by 2100 unlikely. *Nat. Climate Change*, **7**, 637, <https://doi.org/10.1038/nclimate3352>.
- Rajczak, J., and C. Schär, 2017: Projections of future precipitation extremes over Europe: A multimodel assessment of climate simulations. *J. Geophys. Res. Atmos.*, **122**, 10 773–10 800, <https://doi.org/10.1002/2017JD027176>.
- Rasmussen, R., and Coauthors, 2011: High-resolution coupled climate runoff simulations of seasonal snowfall over Colorado: A process study of current and warmer climate. *J. Climate*, **24**, 3015–3048, <https://doi.org/10.1175/2010JCLI3985.1>.
- Sanderson, B. M., K. W. Oleson, W. G. Strand, F. Lehner, and B. C. O'Neill, 2018: A new ensemble of GCM simulations to assess avoided impacts in a climate mitigation scenario. *Climatic Change*, **146**, 303–318, <https://doi.org/10.1007/s10584-015-1567-z>.
- Schulz, K., and M. Bernhardt, 2016: The end of trend estimation for extreme floods under climate change? *Hydrol. Processes*, **30**, 1804–1808, <https://doi.org/10.1002/hyp.10816>.
- Seneviratne, S. I., and Coauthors, 2012: Changes in climate extremes and their impacts on the natural physical environment. *Managing the Risks of Extreme Events and Disasters to Advance Climate Change Adaptation*, C. B. Field et al., Eds., Cambridge University Press, 109–230, https://www.ipcc.ch/site/assets/uploads/2018/03/SREX-Chap3_FINAL-1.pdf.
- Šeparović, L., and Coauthors, 2013: Present climate and climate change over North America as simulated by the fifth-generation Canadian regional climate model. *Climate Dyn.*, **41**, 3167–3201, <https://doi.org/10.1007/s00382-013-1737-5>.
- Sigmond, M., and J. C. Fyfe, 2016: Tropical Pacific impacts on cooling North American winters. *Nat. Climate Change*, **6**, 970–974, <https://doi.org/10.1038/nclimate3069>.
- Sillmann, J., V. V. Kharin, X. Zhang, F. W. Zwiers, and D. Bronaugh, 2013a: Climate extremes indices in the CMIP5 multimodel ensemble: Part 1. Model evaluation in the present climate. *J. Geophys. Res.*, **118**, 1716–1733, <https://doi.org/10.1002/jgrd.50203>.
- , —, F. W. Zwiers, X. Zhang, and D. Bronaugh, 2013b: Climate extremes indices in the CMIP5 multimodel ensemble: Part 2. Future climate projections. *J. Geophys. Res.*, **118**, 2473–2493, <https://doi.org/10.1002/jgrd.50188>.
- Sunyer, M. A., H. J. D. Sørup, O. B. Christensen, H. Madsen, D. Rosbjerg, P. S. Mikkelsen, and K. Arnbjerg-Nielsen, 2013: On the importance of observational data properties when assessing regional climate model performance of extreme precipitation. *Hydrol. Earth Syst. Sci.*, **17**, 4323, <https://doi.org/10.5194/hess-17-4323-2013>.
- Thompson, D. W. J., E. A. Barnes, C. Deser, W. E. Foust, and A. S. Phillips, 2015: Quantifying the role of internal climate variability in future climate trends. *J. Climate*, **28**, 6443–6456, <https://doi.org/10.1175/JCLI-D-14-00830.1>.

- Trenberth, K. E., 1999: Conceptual framework for changes of extremes of the hydrological cycle with climate change. *Weather and Climate Extremes: Changes, Variations and a Perspective from the Insurance Industry*, T. R. Karl, N. Nicholls, and A. Ghazi, Eds., Springer, 327–339.
- , A. Dai, R. M. Rasmussen, and D. B. Parsons, 2003: The changing character of precipitation. *Bull. Amer. Meteor. Soc.*, **84**, 1205–1217, <https://doi.org/10.1175/BAMS-84-9-1205>.
- , and Coauthors, 2007: Observations: Surface and atmospheric climate change. *Climate Change 2007: The Physical Science Basis*, S. Solomon et al., Eds., Cambridge University Press, 235–336.
- Tripathi, O. P., and F. Dominguez, 2013: Effects of spatial resolution in the simulation of daily and subdaily precipitation in the southwestern US. *J. Geophys. Res.*, **118**, 7591–7605, <https://doi.org/10.1002/jgrd.50590>.
- van den Besselaar, E. J. M., A. M. G. Klein Tank, and T. A. Buishand, 2013: Trends in European precipitation extremes over 1951–2010. *Int. J. Climatol.*, **33**, 2682–2689, <https://doi.org/10.1002/joc.3619>.
- van der Linden, P., and J. F. B. Mitchell, Eds., 2009: ENSEMBLES: Climate change and its impacts: Summary of research and results from the ENSEMBLES project. Met Office Hadley Centre, 160 pp., http://ensembles-eu.metoffice.com/docs/Ensembles_final_report_Nov09.pdf.
- Volosciuk, C., D. Maraun, V. A. Semenov, and W. Park, 2015: Extreme precipitation in an atmosphere general circulation model: Impact of horizontal and vertical model resolutions. *J. Climate*, **28**, 1184–1205, <https://doi.org/10.1175/JCLI-D-14-00337.1>.
- von Salzen, K., and Coauthors, 2013: The Canadian Fourth Generation Atmospheric Global Climate Model (CanAM4). Part I: Representation of physical processes. *Atmos.–Ocean*, **51**, 104–125, <https://doi.org/10.1080/07055900.2012.755610>.
- Wang, X. L., and Coauthors, 2011: Trends and low-frequency variability of storminess over western Europe, 1878–2007. *Climate Dyn.*, **37**, 2355–2371, <https://doi.org/10.1007/s00382-011-1107-0>.
- Wehner, M. F., 2013: Very extreme seasonal precipitation in the NARCCAP ensemble: Model performance and projections. *Climate Dyn.*, **40**, 59–80, <https://doi.org/10.1007/s00382-012-1393-1>.
- Westra, S., L. V. Alexander, and F. W. Zwiers, 2013: Global increasing trends in annual maximum daily precipitation. *J. Climate*, **26**, 3904–3918, <https://doi.org/10.1175/JCLI-D-12-00502.1>.
- , and Coauthors, 2014: Future changes to the intensity and frequency of short-duration extreme rainfall. *Rev. Geophys.*, **52**, 522–555, <https://doi.org/10.1002/2014RG000464>.
- Wuebbles, D., and Coauthors, 2014: CMIP5 climate model analyses: Climate extremes in the United States. *Bull. Amer. Meteor. Soc.*, **95**, 571–583, <https://doi.org/10.1175/BAMS-D-12-00172.1>.
- Zhang, X., F. W. Zwiers, G. Li, H. Wan, and A. J. Cannon, 2017: Complexity in estimating past and future extreme short-duration rainfall. *Nat. Geosci.*, **10**, 255, <https://doi.org/10.1038/ngeo2911>.
- Zhu, J., 2013: Impact of climate change on extreme rainfall across the United States. *J. Hydrol. Eng.*, **18**, 1301–1309, [https://doi.org/10.1061/\(ASCE\)HE.1943-5584.0000725](https://doi.org/10.1061/(ASCE)HE.1943-5584.0000725).
- Zolina, O., 2012: Changes in intense precipitation in Europe. *Changes in Flood Risk in Europe*, Z. Kundewicz, Ed., IAHS Press Special Publ. 10, 97–119.
- , C. Simmer, A. Kapala, P. Shabanov, P. Becker, H. Mächel, S. Gulev, and P. Groisman, 2014: Precipitation variability and extremes in central Europe: New view from STAMMEX results. *Bull. Amer. Meteor. Soc.*, **95**, 995–1002, <https://doi.org/10.1175/BAMS-D-12-00134.1>.